CHEMISTRY
A EUROPEAN JOURNAL

DOI: 10.1002/chem.200500142

A Spirocyclic P–S Cage Cation: Synthesis and Formation of $P_7S_6I_2^+$

Marcin Gonsior,[a] Ingo Krossing,*[b] and Eberhard Matern[a]

Abstract: Upon ionization of the $P_4S_3I_2$ molecule with $Ag[Al(OR)_4]$, a highly reactive sulfonium cation $P_4S_3I^+$ is generated (NMR simulated and assigned). At −80 °C this cation reacts with additional $P_4S_3I_2$ to give either an iodophosphonium $P_4S_3I_3^+$ cation (NMR simulated and assigned) and P_4S_3 or to give several isomers of a metastable compound that is probably $P_8S_3I_3^+$. This mixture decomposes at 0 °C to give only three isomers of the spirocyclic $P_7S_6I_2^+$ cage cation (^{31}P NMR simulated and assigned, X-ray of one isomer, IR assigned). The oxidation of the $[Ag(P_4S_3)_2]^+$ complex by I_2 also resulted in the formation of $P_7S_6I_2^+$, but with more by-products. The spirocyclic 15-atom cage of $P_7S_6I_2^+$ has no precedent and contains the first phosphonium center bonded only to P and S atoms. This structural element gives the first experimental clue as to how formal charge-bearing elements in the still unknown class of binary P–Ch (Ch = chalcogen) or homopolyatomic P cations may be constructed.

Keywords: cage compounds · cations · halogens · phosphorus · silver · sulfur

Introduction

Cationic binary P–E or ternary P–E–X cages (E = O–Te; X = halogen) are almost unknown, and the few examples were observed by mass spectrometry.[1] The high reactivity of such phosphorus cations, which are not compatible with anions such as $[SbF_6]^-$ or $[AsF_6]^-$[2,3] (formation of PF_3), may account for this. It appeared likely that such $P_xE_y^+$ or $P_xE_yX_z^+$ species could be isolated given the right counterion. Since the fluorinated $[Al(OR^F)_4]^-$ alkoxyaluminates allowed the synthesis of stable salts of phosphorus-rich cations such as $P_3I_6^+$ and $P_5X_2^+$, it seemed likely that these anions are also suitable for stabilizing $P_xE_y^+$ or $P_xE_yX_z^+$. $Ag[Al(OR^F)_4]$ ($R^F = C(CF_3)_3$),[4] tested in many halide abstraction reactions,[5–11] is a likely starting material to achieve this. Thus by reaction of Ag^+ with PX_3 and P_4S_3, the first[6] ternary $P_5S_3X_2^+$ (**1ab**), $P_5S_2X_2^+$ (**2ab**), and $P_4S_4X^+$ (**3ab**) ions were recently obtained (X = Br, I).

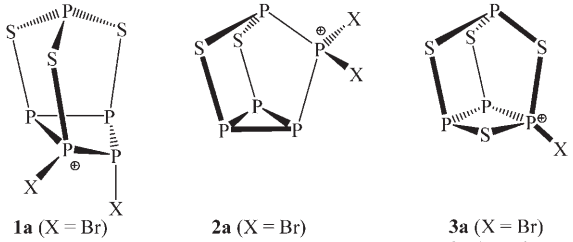

1a (X = Br) **1b** (X = I) **2a** (X = Br) **2b** (X = I) **3a** (X = Br) **3b** (X = I)

Thus, with chemically robust and very weakly coordinating anions[12] the decomposition of reactive P–E–X cations can be avoided. However, the intrinsic stability of a $P–E^+$ or $P–E–X^+$ cage has been little explored. The positive charge in such P–S(–X) cages can formally be localized on a phosphenium (a), sulfonium (b), or phosphonium center ((c) in Figure 1).

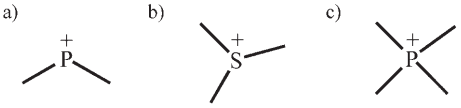

Figure 1. Three possible charge-bearing moieties in the P–S or P–S–X cations: a) phosphenium ion, b) sulfonium ion, c) phosphonium ion.

[a] Dr. M. Gonsior, Dr. E. Matern
Universität Karlsruhe (TH)
Institut für Anorganische Chemie
Engesserstrasse Geb. 30.45, 76128 Karlsruhe (Germany)

[b] Prof. I. Krossing
Ecole Polytechnique Fédérale de Lausanne (EPFL)
Laboratory of Inorganic and Coordination Chemistry (LCIC)
ISIC-BCH, 1015 Lausanne (Switzerland)
E-mail: ingo.krossing@epfl.ch

Supporting information (NMR spectra, simulations, and enlargements of all mentioned compounds; additional tables and figure for X-ray crystallography; *xyz* orientations, vibrational frequencies, total energies, calculated coupling constants, and isotropic shielding tensors; additional structures of the $P_4S_3I^+$ ions; additional IR data including simulation and experimental spectrum, additional text sections on $P_8S_6I_3^+$, and additional experimental details) for this article is available on the WWW under http://www.chemeurj.org/ or from the author.

Since a stable phosphenium ion with only P or S donor ligands is unknown, the PY_2^+ phosphenium ion (Y = P or S donor ligands) is likely the least favorable form of those three structural elements. However, from first principles as well as quantum chemistry[13,14] it is clear that PY_2^+ is less reactive than the PX_2^+ ions (X = halogen), but still much more reactive than the abundant $P(NR_2)_2^+$ aminophosphenium ions. Only a few cations closely related to PY_2^+ are known[15,16] and the only published true PY_2^+ example is the $(H_2CS)_2P^+$ intermediate generated in situ from $AlCl_3$ and cyclic $ClP(SCH_2)_2$.[17] Potentially more stable is the tricoordinate sulfonium cation in Figure 1, but this element is also unknown if only bound to P or S atoms. However, the heavier $As_3S_4^+$ homologue[18] contains such a sulfonium center. Phosphonium cations PR_4^+ with a wide variety of R ligands are abundant but, to the best of our knowledge, no such cation with only P- and S-type ligands is known, whereas a few examples of spirophosphonium cations ligated by four S atoms have been published.[17,19,20] Thus, the properties of compounds including one of the three cationic structural elements in Figure 1, but bonded only to P- and S-type ligands are not very well explored.

Herein we describe the formation of a $P_4S_3I^+$ sulfonium ion as well as the novel spirocyclic $P_7S_6I_2^+$ cage cation with a phosphonium center bonded only to P and S atoms.

Results

Synthesis of the $P_7S_6I_2^+[Al(OR)_4]^-$ salt 4: Crystals of $P_7S_6I_2^+[Al(OR)_4]^-$ (**4**) were first obtained from the reaction between $Ag(P_4S_3)_2^+[Al(OR)_4]^-$ and two equivalents of I_2 carried out in CH_2Cl_2/CS_2 at −78 °C [Eq. (1)].

$$[Ag(P_4S_3)_2]^+[Al(OR)_4]^- + 2\,I_2 \xrightarrow[-78\,^oC]{CH_2Cl_2/CS_2} P_7S_6I_2^+[Al(OR)_4]^- + AgI + \cdots \quad (1)$$

However, Equation (1) is not as selective as our Ag^+/PX_3 = "PX_2^+" reactions[6] leading to **1ab** and in the ^{31}P NMR spectrum of the initial phase of the reaction, many by-products were observed. From this reaction, we also isolated a few crystals of **2b** (unit cell determination) and observed the signals of **1b** and **2b** in the in situ NMR spectrum. Since P_4S_3 reacts with I_2 to give initially only β- and then after melting α-$P_4S_3I_2$,[1,21] we assumed that α- or β-$P_4S_3I_2$ is formed from P_4S_3 and I_2 as the primary step. We also suspected diiodine to be responsible for the destruction of the P_4S_3 cage and the indirect formation of $P_5S_3I_2^+$ and $P_5S_2I_2^+$ among the by-products. We therefore allowed α- and β-$P_4S_3I_2$[21] to react with $Ag[Al(OR)_4]$ (in situ NMR experiments). The reactions were prepared directly before the measurements and kept at −78 °C. In all $P_4S_3I_2$ reactions, AgI precipitated immediately at −78 °C. The signals of two P_4 species were repeatedly observed in the reaction with $P_4S_3I_2$; these signals accounted for 70% of the total intensity. One of these signals is assigned to a short-lived, very reactive $P_4S_3I^+$ ion, the other signal to the slightly more persistent $P_4S_3I_3^+$ ion (see below). In the course of the reaction both ions disappear rapidly. $P_4S_3I^+$, however, is more reactive and its signals disappear first (3 to 4 h). We were not able to determine whether it transforms into $P_4S_3I_3^+$ or is used up by the reaction with $P_4S_3I_2$. If the in situ NMR tube was shaken for about 20 seconds at room temperature and then immediately measured at −80 °C, the signals of $P_4S_3I^+$ and $P_4S_3I_3^+$ had disappeared. At this time, only three groups of complex multiplets in the range between δ = 240 and 210 ppm, δ = 135 and 115 ppm, and δ = 90 and 60 ppm are visible in the spectrum (see Supporting Information). Almost no change was noticed after storage at −80 °C for two weeks. We assume that these lines originate from several isomers of metastable $P_8S_6I_3^+$ (= $P_4S_3I^+ + P_4S_3I_2$). After a week at 0 °C the spectrum changed completely and is almost identical to that of the initially isolated crystalline **4** (three isomers, stable at RT). Reactions (2) to (4) proceed cleanly with only very minor formation of by-products. The most likely reaction path is summarized in Equations (2)–(4).

$$Ag[Al(OR)_4] + 2P_4S_3I_2 \xrightarrow[-78\,^oC]{CH_2Cl_2} P_4S_3I^+[Al(OR)_4]^- + P_4S_3I_3^+[Al(OR)_4]^- + AgI + \ldots? \quad (2)$$

$$\xrightarrow[-78\,^oC]{CH_2Cl_2} \{P_8S_6I_3^+[Al(OR)_4]^- + AgI\} \quad (3)$$

$$\xrightarrow[-30\,^oC\ \text{to}\ 0\,^oC]{CH_2Cl_2} P_7S_6I_2^+[Al(OR)_4]^- + AgI\ \{+\ {}^1/_n(PI)_n\} \quad (4)$$

The entire reaction appears to be independent of the stoichiometry used (one or two equivalents of $P_4S_3I_2$ per equivalent of $Ag[Al(OR)_4]$) and isomer of $P_4S_3I_2$ (α or β). Therefore, we assume that in a 1:1 reaction, unreacted $Ag[Al(OR)_4]$ is left over in solution.

^{31}P NMR data: Prior to discussing the results it should be noted that we describe the spin systems by a reasonably converged data set. The standard deviations for the simulation are on the order of 1 Hz (See Supporting Information). Owing to the sensitivity of the compounds and the unfavorable signal-to-noise ratio, we did not attempt to obtain a higher accuracy of the coupling constants.

NMR spectra of the four P-atomic intermediates: Two species with four P atoms were observed in the initial stages. According to the simulation of the NMR spectra and the calculation of the chemical shifts and coupling constants the two cations are sulfonium $P_4S_3I^+$ and iodophosphonium $P_4S_3I_3^+$ (Figure 2). We were rather astonished to find out that $P_4S_3I_3^+$ was formed. However, this structure is the only one that agrees with the calculated chemical shifts and coupling

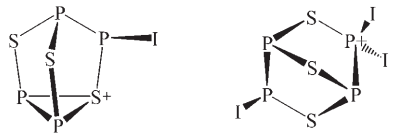

Figure 2. Structures of the $P_4S_3I^+$ sulfonium and $P_4S_3I_3^+$ iodophosphonium cations.

constants (see also Discussion). The NMR data for both intermediates are listed in Table 1.

Comparison of the calculated data for the bromides with the experimental data of the iodides collected in Table 1 shows a very good agreement, if the chemical shifts of halogen-bearing atoms are excluded. For the latter set of atoms, the calculation suffers from the complete neglect of relativistic effects in the calculation; the calculated chemical shifts are systematically in error by about +40 to +90 (one I atom) and +180 to +200 ppm (two I atoms, phosphonium). The most extreme incidence of this behavior was observed for PI_4^+ ($\delta^{31}P_{exp} = -475$ ppm[8]) and attributed to the inverse halogen dependence[24] of the chemical shift of halogen-bearing P atoms. At the MPW1PW91/6–311G(2df) level, the magnitude of the coupling constants ($^1J_{P,P}$) appears to be systematically overestimated by 16 to 42%. However, the $^1J_{P,P}$ couplings are always larger in the calculation than in the experiment.

In Table 1 the chemical shifts and coupling constants of sulfonium $P_4S_3I^+$ are compared with the similar structural units in P_5S_2I[22,23] and $P_5S_2I_2^+$.[6] The agreement between the analogous values is very good and further supports the assignment of the sulfonium structure to $P_4S_3I^+$.

NMR characterization of ***4***: The $P_7S_6I_2^+$ ion found in the crystal structure possesses C_2 symmetry. The spectra of the isolated crystals of **4** as well as those of all in situ reactions [Eqs. (2)–(4)] leading to **4** showed, however, a more complicated situation than expected. Four sets of multiplets between $\delta = +255$ and +245 ppm, $\delta = +193$ and +158 ppm, $\delta = +125$ and +120 ppm, and $\delta = +105$ and +96 ppm were observed (see Supporting Information) and the ^{31}P resonances are assigned to three different isomers. This was particularly visible for the three sets of multiplets centered at $\delta = +249$ ppm (Figure 3).

The signals were assigned to three isomers of a P_7 species in a relative ratio of about 6:4:1. All spectra were recorded at different temperatures between −80 °C and +25 °C but, in contrast to our experience with other P–X and P–S–X systems, no dynamic exchange was observed. Therefore, the skeleton of the $P_7S_6I_2^+$ isomers remains rigid in solution at these temperatures. With this observation, conformational isomerism of the P–I bond was excluded as a possible reason for the presence of three $P_7S_6I_2^+$ isomers. However, if one evaluates the possible arrangements of the $P_4S_3I^+$ unit in **4**, characterized by an X-ray crystal structure, only three different isomers can be envisioned: two C_2-symmetric and one asymmetric isomer (see insets in Figure 3). In isomer I the adjacent sulfur atom of one cage is *exo* to the other cage, and the adjacent phosphorus atom is *endo*, while in isomer III the adjacent phosphorus atom is *exo* and the sulfur atom is *endo*. In isomer II one cage has the adjacent sulfur atom *exo* to it and the other cage has the adjacent phosphorus *exo* to it. Room-temperature 2D $^{31}P/^{31}P$ NMR spectra both in CD_2Cl_2 and in $C_6H_5CF_3$ solution were re-

Table 1. Experimental (X = I) and calculated[a] (X = Br) ^{31}P NMR data of sulfonium $P_4S_3X^+$ in comparison to the related NMR data of P_5S_2I[22] and $P_5S_2I_2^+$.[6] For the assignment of P_A to P_E, see below. NMR data of the nonassigned P_4-intermediate are also shown.

	Calcd[a] $P_4S_3Br^+$ Sulfonium	Exptl $P_4S_3I^+$ 193 K sulfonium	Exptl P_5S_2I[22,23]	Calcd[a] P_5S_2Br[6]	Exptl $P_5S_2I_2^+$[6]	Calcd[a] $P_5S_2Br_2^+$[6]		Exptl $P_4S_3I_3^+$ 193 K	Calcd[a] $P_4S_3Br_3^+$
$\delta(P_A)$	+246[b]	+165.4	+111.35	+200[b]	+61.5	+265	$\delta(P_A)$	+33.0	+210[b]
$\delta(P_B)$	+82	+79.7	+29.91	+46	+21.0	+22	$\delta(P_B)$	+128.3	+112
$\delta(P_C)$	+44	+58.2	−57.33	−51	−45.7	−34	$\delta(P_C)$	+122.5	+164[b]
$\delta(P_D)$	+84	+72.4	−72.08	−76	−45.7	−34	$\delta(P_D)$	+158.9	+176
$\delta(P_E)$	–	–	−200.24	−224	−267.3	−313			
$^1J_{A,B}$	−274	−235.3[c]	−251.52	−323	−370.2[c]	−526	$^1J_{A,B}$	−434.6[c]	−679
$^2J_{A,C}$	+3	14.1	17.03	+3	10.5	−45	$^2J_{A,C}$	18.4	−23
$^2J_{A,D}$	−21	6.2	−8.51	−23	10.5	−45	$^2J_{A,D}$	3.0	−52
$^1J_{A,E}$	–	–	−368.17	−463	−553.7	−772	$^2J_{B,C}$	44.3	+46
$^2J_{B,C}$	+91	84.1	72.75	+63	74.2	+77	$^2J_{B,D}$	84.4	+82
$^2J_{B,D}$	+74	67.2	60.28	+57	74.2	+77	$^1J_{C,D}$	−228.1[c]	−261
$^2J_{B,E}$	–	–	45.51	+42	−4.4	−26			
$^1J_{C,D}$	−229	−197.1[c]	−188.58	−238		−212			
$^1J_{C,E}$	–	–	−169.08	−209	−162.3	−195			
$^1J_{D,E}$	–	–	−168.05	−214	−162.3	−195			

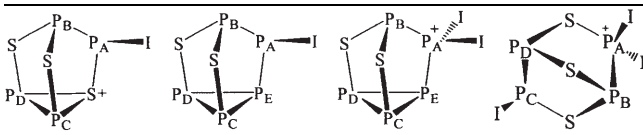

[a] Calculated values were obtained at the MPW1PW91/6–311G(2df) level and are given for the bromides, which are less affected by relativity than the iodides. [b] The calculation of the chemical shift of these atoms suffers from the complete neglect of relativistic effects and should be in error by about +40 to +90 ppm (one iodine atom) or about +180 to +200 ppm (two iodine atoms, phosphonium). [c] A negative sign is assigned to all $^1J_{P,P}$. The signs for the other coupling constants were checked, but are only given if a significant change in the simulated spectra could be observed.

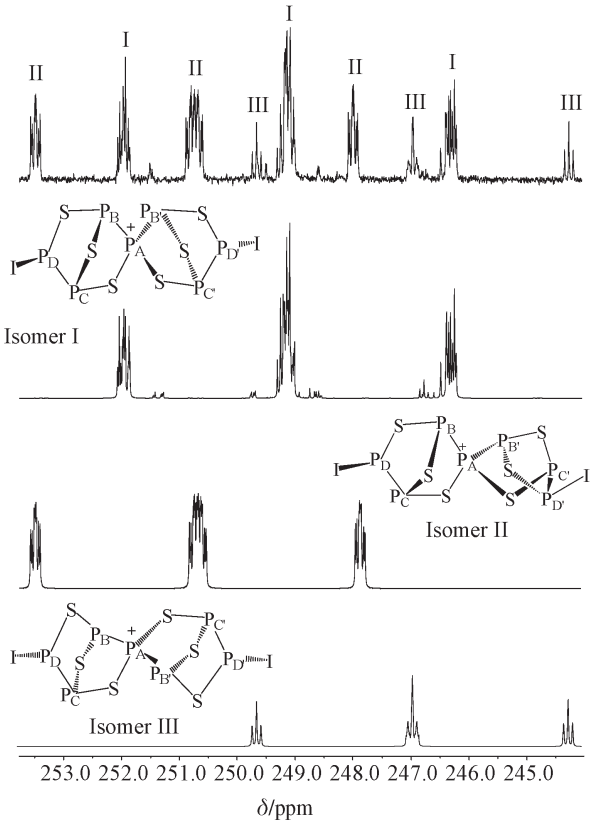

Figure 3. ^{31}P NMR resonances of the P_A atom of the three observed isomers of **4** (top) and their simulations below. The chemical shift scale is shown in ppm. The P atoms in the structures of isomers I, II, and III are labeled according to the assignment in Table 2.

corded to resolve the puzzling coupling patterns, since the signals of the isomers were overlapping, in particular, the multiplets at $\delta = +122$ and $+100$ ppm (see Supporting Information). The spectra of all three isomers were simulated (see Supporting Information) and the chemical shifts and coupling constants are listed in Table 2 together with the calculated chemical shifts of the bromides in the same structure.

The most abundant species is the C_2-symmetric cation in **4** (isomer I). The second most abundant $P_7S_6I_2^+$ ion (isomer II) has no symmetry, and the lowest concentration is found for another C_2-symmetric species (isomer III). Comparison of the calculated chemical shifts of the bromides and the experimental shifts of the iodides in Table 2 shows very good agreement, again if one neglects the shifts of the halogen-bearing atoms that are affected by relativistic effects.[24] This is very evident if one compares the shifts of the P atoms C and C′; the chemical shifts of these structurally rather similar P atoms changes a lot even within one isomer, for example, δ(C/C′) = +191.8 (I), +159.2 and +179.2 (II), +164.7 ppm (III) (in CD_2Cl_2). This is reproduced by the calculations which give: δ(C/C′) = +197.4 (I), +165.2 and +191.9 (II), +172.9 ppm (III). The very good agreement further supports our assignment of the structures of the three isomers of the $P_7S_6I_2^+$ ion.

Crystal structure: Compound **4** crystallized at −28 °C from a very concentrated "oily" solution in the triclinic space group $P\bar{1}$ ($Z = 2$) as yellow, highly air- and moisture-sensitive plates. Two independent molecules are included with the asymmetric unit as well as the cocrystallized solvent molecules CH_2Cl_2 and CS_2 (see Supporting Information). Since one of the two $P_7S_6I_2^+$ ions is disordered over two positions, only the parameters of the ordered cation, which adopts the structure of isomer I in Figure 3, will be discussed.

The cation in **4** can be described as two P_4S_3I units, linked by a common spiro-phosphonium atom (Figure 4). It is nearly C_2-symmetric and the equivalent distances are the

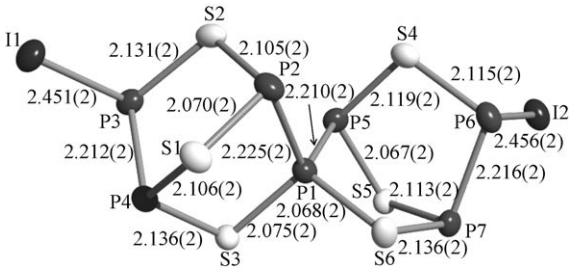

Figure 4. The novel $P_7S_6I_2^+$ ion in the salt **4** (isomer I). For clarity, the $[Al(OR)_4]^-$ ion and the second disordered cation are not shown (see Supporting Information).

same to within 0.003 to 0.016 Å. They were also reproduced by the MP2/TZVPP ab initio calculation (Table 3). The environment around the phosphonium center is nearly ideally tetrahedral (range: 108.38(5)°–111.10(5)°). The $P_7S_6I_2^+$ ion is a unique example of a phosphorus sulfur cage, which contains as many as seven P atoms. This is the highest number of P atoms of all phosphorus sulfur cages known to date. The average P–I bond lengths in **4** (2.454(2) Å) are slightly shorter than in neutral α-$P_4S_3I_2$ (2.474(3) Å), PI_3 (2.461(3) Å) or P_2I_4 (2.472(2) Å). However, they are slightly elongated relative to smaller iodophosphorus cations such as PI_4^+ (2.3700(4) Å, in $PI_4^+[Al(OR)_4]^-$),[8] $P_2I_5^+$ (from 2.399(9)–2.420(9) Å, in $P_2I_5^+[AlI_4]^-$), and $P_3I_6^+$ (from 2.361(6)–2.435(6) Å, in $P_3I_6^+[(RO)_3Al{-}F{-}Al(OR)_3]^-$).[9] The P–P (2.210(2)–2.225(2) Å) and P–S bond lengths (2.067(2)–2.136(2) Å) in **4** are in the typical range for phosphorus sulfides (see Table 3). To the best of our knowledge, no structure with a phosphonium center in an environment of only P and S atoms is known. In spirophosphonium cations, in which the central P atom is surrounded by four S atoms, like in $P(S_2(CH_2)_2)_2^+$ or $P(S_2(CH_2)_3)_2^+$, the P–S distances (av 2.052(2) Å) are by 0.015 Å shorter than the lower limit of the P–S bonds in **4**. This indicates less π-donation of the attached S atoms and/or more efficient charge delocalization around the entire cation in **4**.[20] Both independent $[Al(OR)_4]^-$ anions have an almost tetrahedral geometry, which is slightly affected by librational motion (see Supporting Information).

*The disorder of one of the cations in **4***: The second disordered $P_7S_6I_2^+$ ion (34 % occupation) represents the structure

Table 2. Calculated and experimental ^{31}P NMR data of the three isomers of $P_7S_6X_2^+$.[a]

	$P_7S_6Br_2^+$ calcd (MPW1PW91/6–311G(2df)[b]			$P_7S_6I_2^+$ in CD_2Cl_2			$P_7S_6I_2^+$ in $C_6H_5CF_3$[d] (capillary with $[D_8]$THF)		
	isomer I	isomer II	isomer III	isomer I	isomer II	isomer III	isomer I	isomer II	isomer III
$\delta(P_A)$	+250.1	+250.4	+247.2	+249.1	+250.7	+246.9	+248.7	+251.5	+248.1
$\delta(P_B)$	+116.3	+94.6	+88.9	+123.4	+102.5	+98.3	+119.0	+96.5	+92.3
$\delta(P_{B'})$	+116.3	+94.1	+88.9	+123.4	+100.1	+98.3	+119.0	+93.2	+92.3
$\delta(P_C)$	+197.4	+165.2	+172.9	+191.8	+159.2	+164.7	+190.1	+154.8	+161.8
$\delta(P_{C'})$	+197.4	+191.9	+172.9	+191.8	+179.2	+164.7	+190.1	+176.1	+161.8
$\Delta(P_D)$	+166.6[c]	+170.5[c]	+164.5[c]	+121.6	+124.4	+121.1	+113.7	+118.2	+113.0
$\Delta(P_{D'})$	+166.6[c]	+166.6[c]	+164.5[c]	+121.6	+122.7	+121.1	+113.7	+115.6	+113.0
$^1J_{A,B}$	–	–	–	−455.5	−433.8	−436.0			
$^2J_{A,C}$	–	–	–	5.4	3.9	1.2			
$^3J_{A,D}$	–	–	–	−17.3	11.9	12.5			
$^1J_{A,B'}$	–	–	–	−455.5	−453.3	−436.0			
$^2J_{A,C'}$	–	–	–	5.4	0.0	1.2			
$^3J_{A,D'}$	–	–	–	−17.3	10.3	12.5			
$^2J_{B,C}$	–	–	–	76.0	86.1	81.5			
$^2J_{B,D}$	–	–	–	42.8	40.1	49.0			
$^2J_{B,B'}$	–	–	–	16.5	15.6	−16.9			
$^3J_{B,C'}$	–	–	–	−3.9	1.4	−1.9			
$^4J_{B,D'}$	–	–	–	−7.1	−6.9	4.0			
$^1J_{C,D}$	–	–	–	−234.4	−226.8	−230.4			
$^3J_{C,B'}$	–	–	–	−3.9	−7.1	−1.9			
$^4J_{C,C'}$	–	–	–	0.0	0.0	0.0			
$^5J_{C,D'}$	–	–	–	0.0	0.0	−1.5			
$^4J_{D,B'}$	–	–	–	−7.1	8.1	4.0			
$^5J_{D,C'}$	–	–	–	0.0	0.0	−1.5			
$^6J_{D,D'}$	–	–	–	0.0	0.0	0.0			
$^2J_{B',C'}$	–	–	–	76.0	77.2	81.5			
$^2J_{B',D'}$	–	–	–	42.8	47.7	49.0			
$^1J_{C',D'}$	–	–	–	−234.4	−226.2	−230.4			

[a] For an assignment of the atoms, see Figure 4. [b] With all attempts the calculation collapsed after giving the shielding tensors and we were not able to obtain the calculated coupling constants of this system. [c] The calculated chemical shifts of these halogen-bearing atoms are most strongly affected by the complete neglect of relativistic effects and are therefore in error by about +40 to +50 ppm. [d] Coupling constants were not optimized owing to an unfavorable signal-to-noise ratio. Using the solvent shift differences to CD_2Cl_2 the chemical shifts for all P atoms could be identified in both data sets in spite of some superimposed multiplets.

Table 3. Experimental and calculated bond lengths of the $P_7S_6I_2^+$ cation (isomer I). For equivalent bonds only the average lengths are given (full list in the Supporting Information).

$P_7S_6I_2^+$	Experiment	Calculation[a]	α-$P_4S_3I_2$
I1(2)–P3(6)	2.454(2)	2.431	2.474(3)
P1–S6(3)	2.072(2)	2.081	2.115(3)
P1–P5(2)	2.218(2)	2.237	2.207(4)
P2(5)–S1(5)	2.069(2)	2.085	2.090(3)
P2(5)–S2(4)	2.112(2)	2.122	2.132(3)
P3(6)–S2(4)	2.123(2)	2.147	2.115(3)
P3(6)–P4(7)	2.214(2)	2.211	2.208(4)
P4(7)–S1(5)	2.110(2)	2.122	2.099(4)
P4(7)–S3(6)	2.136(2)	2.155	2.129(3)

[a] MP2/TZVPP.

of Isomer III (see NMR section). The main occupation on this site is Isomer I, which is also found at the nondisordered $P_7S_6I_2^+$ site. It thus appears that Isomer III cocrystallizes with Isomer I and partially replaces it (see Supporting Information). Because of the disorder, the structural parameters of both isomers residing on the disordered site are not reliable and cannot be used for the discussion. However, this observation confirmed the proposed structure of the second C_2-symmetric $P_7S_6I_2^+$ ion.

Cation–anion contacts, charge distribution, and solid-state packing of ***4***: The phosphonium center in **4** shows no contacts with the counterion below 4.269 Å. All atoms apart from P3, P4, P6, and S4 exhibit weak contacts to fluorine (Figure 5). The strongest interaction was found for S1···F66 at 2.812 Å, while all other P···F or S···F distances are longer than 3.0 Å. We used the empirical formula devised by I. D. Brown to calculate the partial charges residing on the sulfur atoms in **4** from the number and lengths of the fluorine contacts.[25] The experimentally estimated partial charges together with the results of population analyses of the calculated structures (MP2 and BP86 level) are summarized in Table 4.

We conclude from Table 4 that the charge distribution in an ionic species obtained by a population analysis (with ab initio or DFT methods) may be inconsistent with the values obtained experimentally from solid-state fluorine contacts. The experiment clearly shows that almost half of the positive charge resides on the S atoms while the computations even assign negative partial charges to the S atoms. This is in agreement with earlier observations.[5,6,8,11]

IR spectroscopy: We recorded IR spectra of crystalline **4**. To assign the vibrations of the cations, frequency calcula-

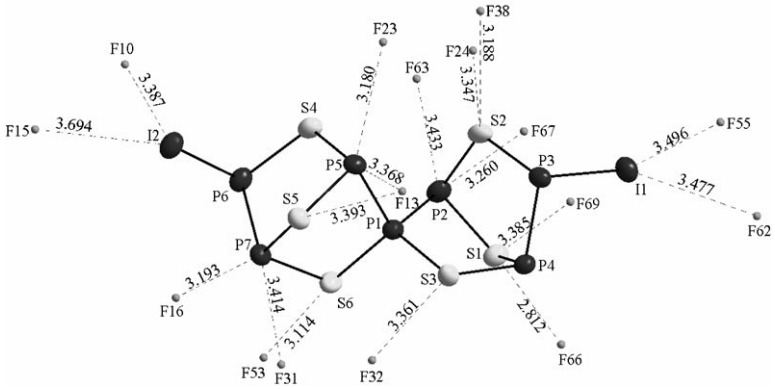

Figure 5. Fluorine contacts of the cation in **4** below the van der Waals limit.

Table 4. Charge distribution in the $P_7S_6I_2^+$ ion (isomer I).

Atom	number of F contacts	Exptl charge	MP2-calcd[a] charge	BP86-calcd[a] charge
P1	0		+0.65	+0.33
P2	2		+0.22	+0.19
P3	0		+0.12	+0.14
P4	0		+0.22	+0.16
P5	2		+0.22	+0.19
P6	0		+0.12	+0.14
P7	2		+0.22	+0.16
S1	2	+0.16	−0.09	−0.02
S2	2	+0.12	−0.15	−0.10
S3	1	+0.05	−0.14	−0.06
S4	0		−0.15	−0.10
S5	1	+0.05	−0.09	−0.02
S6	1	+0.07	−0.14	−0.06
I1	2		0.00	+0.03
I2	2		0.00	+0.03

[a] Paboon = Population analysis based on occupation numbers; TZVPP basis for MP2 and SVP basis for BP86 calculation.

tions were carried out at the BP86/SV(P) level. Although the measurement was likely carried out on a sample containing all three isomers of $P_7S_6I_2^+$, the spectrum is assigned only taking the most abundant Isomer I into consideration. We carried out frequency calculations for all three isomers. However, the vibrations of all the isomers are almost equal in energy and intensity (see Supporting Information). Therefore, we have no additional IR spectroscopic evidence for the three isomers found in solution. The spectrum was simulated by a superposition of Gauss functions using the calculated frequencies and intensities of the cation and $[Al(OR)_4]^-$ and was compared with the experimental as well as a simulated spectrum of the anion (see Supporting Information). The absorptions of $P_7S_6I_2^+$ appear in the far infrared below 600 cm^{-1}. Since it consists of two (α)-P_4S_3I fragments, the vibrations of α-$P_4S_3I_2$ appear in a similar region to those of $P_7S_6I_2^+$ (see Table 5 and Supporting Information). Cocrystallized CS_2 was also observed in the spectrum of **4** (cf. gaseous CS_2: ν_3 = 1533 cm^{-1}).[26] The vibrations of $[Al(OR)_4]^-$ were clearly assigned by comparison to known salts (Table 5). However, the anion bands differ slightly from the known pattern, probably because of lattice splitting. The area of the $C(CF_3)_3$ vibrations between 1021 and 1354 cm^{-1} is unusually broad. This is in agreement with the presence of two nonequivalent anions in the crystal lattice. The 830 cm^{-1} anion band splits to 809 and 868 cm^{-1}. Similarly, the spectra of the solvent-free Ag-$[Al(OR)_4]$ (796, 827, 862 cm^{-1}) and Li$[Al(OR)_4]$ (800, 825, 863 cm^{-1}) show this pattern to an even higher degree.[27]

Discussion

Thermodynamic quantities given in the following discussion approximate $\Delta G°$ in CH_2Cl_2 at 298 K and were taken from the MP2/TZVPP calculations that include approximate solvation free energies obtained by the COSMO model. Details of ΔH(0 K, g), $\Delta G°$(g), and $\Delta G°(CH_2Cl_2)$ data for all reactions mentioned in the text is available in the Supporting Information.

The formation of the $P_4S_3I^+$ sulfonium cation: $P_4S_3I^+$ is likely formed by the interaction of the dissolved Ag-$(CH_2Cl_2)_3^+$ ion with the iodine atom of α-$P_4S_3I_2$; Figure 6 rationalizes its formation. In fact, this appears to be a HOMO–LUMO interaction of the HOMO of α-$P_4S_3I_2$ (mainly at iodine; −6.428 eV) with the LUMO of Ag-$(CH_2Cl_2)_3^+$ (Ag $5s^0$; at −6.149 eV; orbitals deposited). It is likely that upon ionization of the P–I bond by Ag^+ the new P–S bond and with it the nortricyclane cage is formed. The assignment of a sulfonium structure to this $P_4S_3I^+$ ion is in agreement with the known structure of $As_3S_4^+$,[18] which is isoelectronic and isolobal (Figure 7).

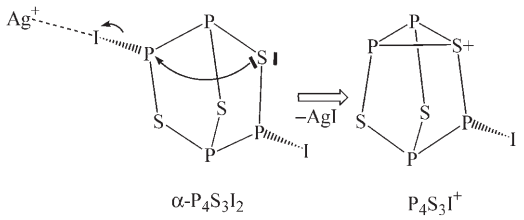

Figure 6. Likely formation of $P_4S_3I^+$.

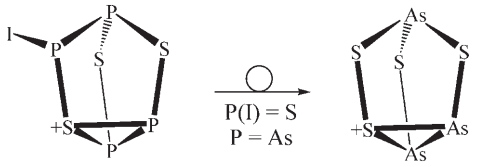

Figure 7. Relation of the structures of sulfonium $P_4S_3I^+$ and $As_3S_4^+$.[18]

Table 5. Experimental IR bands of **4** [cm^{-1}]. Assignment of the cation vibrations based on the α-$P_4S_3I_2$ Raman modes and the BP86/SVP calculated frequencies.

4 IR	$P_7S_6I_2^+$ calcd[a] (Int. [km mol^{-1}])	**4** assignment	α-$P_4S_3I_2$ RA exptl (calcd)	IR $[Al(OR)_4]^-$ [b]
219 (w)		$[Al(OR)_4]^-$		215 (w)
230 (m)	223 (19)	δ(P–S–P)	229 (223)	
	224 (5)			
261 (w)	247 (3)	δ_s(S–P–P)	259 (258)	
286 (m)		$[Al(OR)_4]^-$		284 (w)
	272 (0), 302 (6)			
	304 (1), 317 (4)			
314 (s)		$[Al(OR)_4]^-$		314 (w)
321 (m)	318 (18), 329 (2)	ν_{as}(P–I)	318 (291)	
335 (m)	344 (41)	ν_{as}(P–S)	340 (319)	330 (vw)
368 (m)		$[Al(OR)_4]^-$		
379 (m)		$[Al(OR)_4]^-$		
402 (s)	351 (228)	ν_{as}(P–S–P)	406 (388)	
	357 (8), 365 (7)			365 to 427 (br.)
	369 (1), 371 (2)			
422 (s)	382 (78)	ν_{as}(IP–PS)	413 (392)	
	384 (4), 410 (0)			
436 (s)	412 (11), 417 (1)	ν_{as}(S–P–P)	444 (414)	
444 (s)		$[Al(OR)_4]^-$		445 (m)
491 (m)	458 (32), 461 (6)	ν_{as}(P_{ph}P–S)[c]	484 (456)	
523 (sh)	470 (5), 475 (71)	ν_s(P_{ph}P–S)[c]		
536 (s)		$[Al(OR)_4]^-$		537 (mw)
560 (m)		$[Al(OR)_4]^-$		561 (mw)
571 (m)		$[Al(OR)_4]^-$		571 (w)
728 (s)		$[Al(OR)_4]^-$		728 (s)
755 (m)		$[Al(OR)_4]^-$		755 (w)
809 (m)		$[Al(OR)_4]^-$		
828 (m)		$[Al(OR)_4]^-$		832 (m)
868 (w)		$[Al(OR)_4]^-$		
975 (vs)		$[Al(OR)_4]^-$		973 (vs)
1021 (m)		$[Al(OR)_4]^-$		
1100 (s)		$[Al(OR)_4]^-$		1075 (sh)
1134 (s)		$[Al(OR)_4]^-$		1133 (sh)
1148 (s)		$[Al(OR)_4]^-$		
1163 (s)		$[Al(OR)_4]^-$		1169 (ms)
1221 (vs)		$[Al(OR)_4]^-$		1219 (vs)
1248 (vs)		$[Al(OR)_4]^-$		1242 (vs)
1260 (vs)		$[Al(OR)_4]^-$		
1275 (vs)		$[Al(OR)_4]^-$		1276 (vs)
1300 (s)		$[Al(OR)_4]^-$		1301 (s)
1354 (m)		$[Al(OR)_4]^-$		1353 (ms)
1517 (m)		CS_2		
1523 (m)		CS_2		

[a] Calculated low-frequency vibrations of $P_7S_6I_2^+$: 15(0), 16(0), 36(0), 50(0), 56(0), 56(0), 60(1), 84(0), 112(0), 122(0), 123(2), 137(2), 160(0) cm^{-1} (calcd IR int.); [b] The frequencies of $[Al(OR)]_4^-$ are compared with those of $CS_2Br_3^+[Al(OR)]_4^-$. [c] P_{ph} = phosphonium P atom.

This assignment is also in agreement with the thermodynamics calculated to be exergonic by −183 kJ mol^{-1}, if the formation of solid AgI is assumed [Eq. (5)].

$$\alpha\text{-}P_4S_3I_{2(solv)} + Ag(CH_2Cl_2)_3^+{}_{(solv)} \xrightarrow[\Delta G^\circ_{AgI(s)} = -183\ kJ\ mol^{-1}]{\Delta G^\circ_{AgI(solv)} = +14\ kJ\ mol^{-1}} P_4S_3I^+{}_{(solv)} + AgI_{(solv)/(s)} + 3CH_2Cl_{2(solv)} \quad (5)$$

The assigned sulfonium $P_4S_3I^+$ is the global minimum of all 25 assessed $P_4S_3I^+$ isomers. The formation of this sulfonium $P_4S_3I^+$ with two separated P_2 units also suggests that ionization only starts from α-$P_4S_3I_2$, regardless of whether α- or β-$P_4S_3I_2$ was used initially (β-$P_4S_3I_2$ contains a P_3 chain). Additional experimental evidence for the instability of the $P_4S_3I^+$ cations formed from β-$P_4S_3I_2$ followed from mass spectrometry:[1] Ionization starting from pure α-$P_4S_3I_2$ showed that the $P_4S_3I^+$ ion has a high relative intensity of 100%. When starting from the β-isomer, the signal due to the $P_4S_3I^+$ ion was of low relative intensity (6%).[1] This indicates that the $P_4S_3I^+$ cations formed more readily from the α- than from the β-form. Accordingly (α)-$P_4S_3I^+$ is likely more stable in the gas phase than (β)-$P_4S_3I^+$. These findings and the presence of two four P-atomic cations with two separated P_2 units in the in situ NMR suggest that β-$P_4S_3I_2$ with a P_3 unit is isomerized to α-$P_4S_3I_2$ with two P_2 units before the reaction. This may proceed upon complexation to Ag^+ and prior to ionization. Such an isomerization is exergonic by −5 kJ mol^{-1} [Eq. (6)].

$$\beta\text{-}P_4S_3I_{2(solv)} \longrightarrow \alpha\text{-}P_4S_3I_{2(solv)} \quad (6)$$
$$\Delta G^\circ_{CH_2Cl_2} = -5\ kJ\ mol^{-1}$$

Such an isomerization would also easily explain the formation of the sulfonium $P_4S_3I^+$ from both β-$P_4S_3I_2$ and α-$P_4S_3I_2$.

Alternative $P_4S_3I^+$ structures and the formation of $P_4S_3I_3^+$: Figure 8 shows the four lowest energy structures of the $P_4S_3I^+$ ions derived from α-$P_4S_3I_2$.[28] Despite computationally assessing 25 isomers of the $P_4S_3X^+$ cations, we were not able to match the NMR data of the second four P-atomic species with the calculated chemical shifts and coupling constants. One of the referees then suggested that this compound is in fact not another $P_4S_3I^+$ ion, but rather a $P_4S_3I_3^+$ ion, which is related to α-$P_4S_3I_2$ (β-$P_4S_3I_2$ is impossible, since it has a P_3 unit). If one formally adds an "I^+" ion to one of the two equivalent P(I) atoms of α-$P_4S_3I_2$, this leads to the $P_4S_3I_3^+$ structure shown in Figure 9.

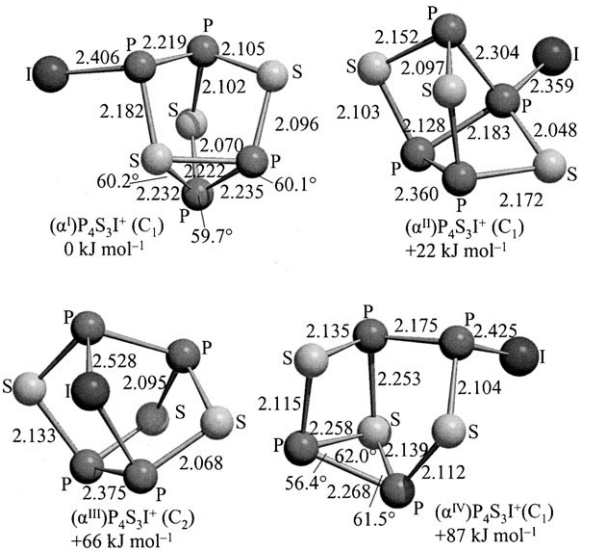

Figure 8. MP2/TZVPP minimum structures calculated for the $P_4S_3I^+$ ions derived from α-$P_4S_3I_2$. The relative energies in solution ($\Delta G°_{CH2Cl2}$) are given.

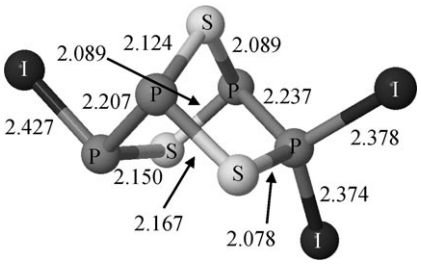

Figure 9. MP2/TZVPP structure of $P_4S_3I_3^+$ (distances in Å).

In fact the calculated chemical shifts and coupling constants for this compound are in excellent agreement with the experimental data in Table 1 (see above). Thus we have to conclude that in the initial stages of the reaction a $P_4S_3I_3^+$ cation is also formed and is present in solution longer than the sulfonium $P_4S_3I^+$. Its formation is assessed in the next section.

Formation of the spirocyclic $P_7S_6I_2^+$ cation: The first step for $P_7S_6I_2^+$ formation by the $Ag(P_4S_3)_2^+/I_2$ route is the slow oxidation of P_4S_3 to $P_4S_3I_2$ [Eq. (7)].

$$P_4S_{3(solv)} + I_{2(solv)} \longrightarrow \alpha,\beta\text{-}P_4S_3I_{2(solv)} \qquad (7)$$

α, $\Delta G° = -44$ kJ mol^{-1}
β, $\Delta G° = -39$ kJ mol^{-1}

The slowly formed (Ag^+-coordinated?) $P_4S_3I_2$ may immediately react with Ag^+ giving $P_4S_3I^+$ or $P_4S_3I_3^+$ and then react with further available substrates. Owing to the abundance of several competing I_2, P_4S_3, or $P_4S_3I_2$ substrates for $P_4S_3I^+$ or $P_4S_3I_3^+$, this reaction is less clean than those using only $P_4S_3I_2$ as a starting material. Hence we also observed the formation of **1b** and **2b** by NMR. However, once $P_4S_3I_2$ is formed, both reactions proceed analogously to give **4**.

Starting with $P_4S_3I^+$ and α-$P_4S_3I_2$, the formation of $P_7S_6I_2^+$ probably proceeds according to the two hypothetical pathways as sketched in Scheme 1. This mechanism is in agreement with all available experimental data and especially the observation that the $P_4S_3I_3^+$ formed in situ is much longer-lived than sulfonium $P_4S_3I^+$. Moreover it is in agreement with the calculated Gibbs energies in solution. In a major pathway, the interaction of sulfonium $P_4S_3I^+$ with α-$P_4S_3I_2$ would give the proposed $P_8S_6I_3^+$ intermediate (= $P_4S_3I^+$ *$P_4S_3I_2$) that is metastable at −78 °C. Analogously to **1a** and **1b**,[6] this $P_8S_6I_3^+$ intermediate likely stabilizes itself by the irreversible separation of PI, probably as P_6I_6. Alternatively the reaction of sulfonium $P_4S_3I^+$ with α-$P_4S_3I_2$ may also lead to $P_4S_3I_3^+$ and P_4S_3. Since the $P_4S_3I_3^+$ ion contains a charged P^+I_2 unit, it is likely that it may react with the iodide of another α-$P_4S_3I_2$ molecule by formation of PI_3 and $P_7S_6I_2^+$. The by-products P_4S_3 and PI_3 are insoluble in CD_2Cl_2 at low temperature and therefore not visible in the ^{31}P NMR. However, they are known[21b] to react and produce α-$P_4S_3I_2$, which then re-enters the cycle. Both pathways lead cleanly to $P_7S_6I_2^+$ and "PI" (as P_6I_6) with no other by-products, as seen in the experiment.

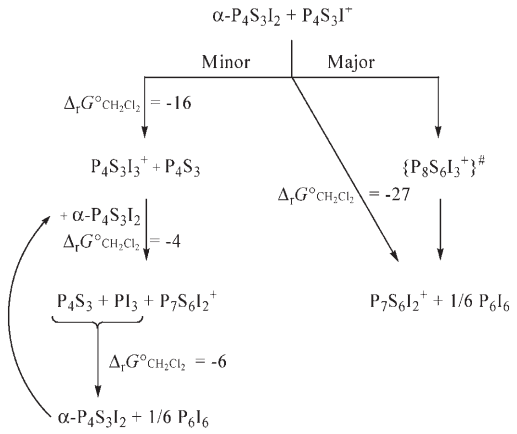

Scheme 1. Hypothetical pathways for the formation of $P_7S_6I_2^+$ from $P_4S_3I^+$ and α-$P_4S_3I_2$. The Gibbs energies in solution were calculated at the MP2/TZVPP level with inclusion COSMO solvation enthalpies.

The overall formation of $P_7S_6I_2^+$ as in Equation (8) is exergonic even if only the formation of dissolved AgI is assumed. $P_7S_6I_2^+$ in Equation (8) adopts the conformation as found in the X-ray structure of **4**.

$$2\ \alpha\text{-}P_4S_3I_{2(solv)} + Ag(CH_2Cl_2)_3^+{}_{(solv)} \xrightarrow[\Delta G°_{AgI(s)} = -195\ kJ\ mol^{-1}]{\Delta G°_{AgI(solv)} = -12\ kJ\ mol^{-1}} P_7S_6I_2^+{}_{(solv)} + AgI_{(solv)/(s)} + 1/6\ P_6I_6 + 3\ CH_2Cl_{2(solv)} \qquad (8)$$

*Isomers of the $P_7S_6I_2^+$ cation in **4***: The three $P_7S_6I_2^+$ isomers shown in Figure 10 were observed by NMR spectroscopy.

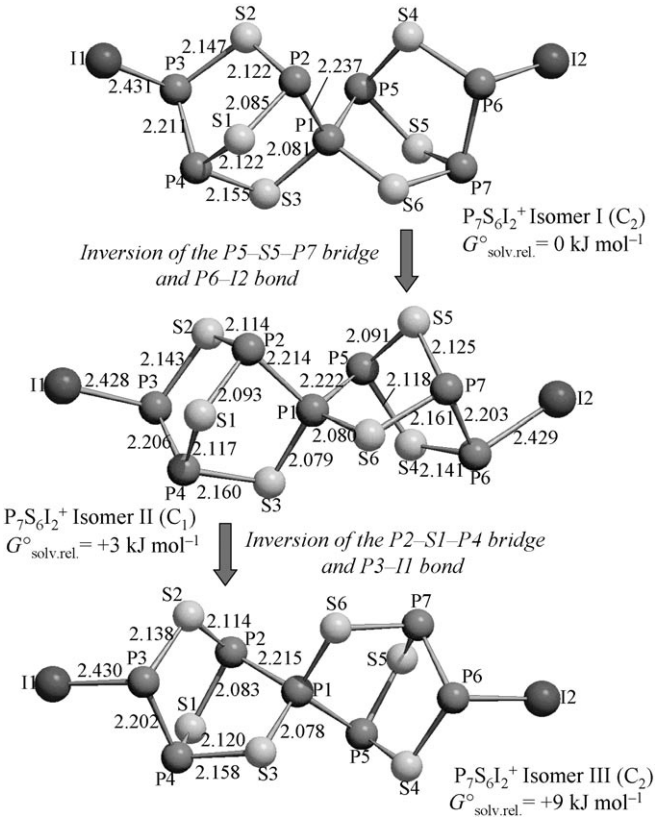

Figure 10. The three isomers I, II, and III of the $P_7S_6I_2^+$ cation are accompanied by their enantiomers (not shown; calculation: MP2/TZVPP). The differences of isomer II and III with respect to isomer I may be understood by the formal transformations written next to the grey arrow.

The relative intensities of these isomers (6:4:1) are in agreement with the calculated relative energies in Figure 10. The structure of Isomer III was also observed as part of the disordered cation position in the crystal structure of **4**.[29] Figure 10 rationalizes the changes in structure between the isomers.

Conclusion

The reaction between $Ag(P_4S_3)_2^+[Al(OR)_4]^-$ and I_2 as well as α- or β-$P_4S_3I_2$ led to a mixture of three isomers of the $P_7S_6I_2^+$ spiro-phosphonium cation with a unique tetracoordinate phosphonium center bonded only to P and S atoms. A sulfonium $P_4S_3I^+$ ion with nortricyclane structure, formed from $P_4S_3I_2$ and Ag^+, and an iodophosphonium $P_4S_3I_3^+$ ion, formed from $P_4S_3I_2$ and $P_4S_3I^+$, are the key intermediates.

We learned from this work that finding the right precursor could be the key to the synthesis of the hitherto still unknown class of homopolyatomic P_n^+ cations (n = any number). The structure of **4** shows that likely P_n^+ structures should contain a tetracoordinate phosphonium center that formally bears the positive charge. From this perspective, the most likely calculated isomer of P_n^+ to be realized is the P_9^+ structure shown in Figure 11 (global minimum of the P_9^+ PES).[30]

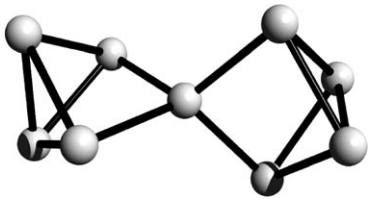

Figure 11. Calculated global minimum structure of P_9^+.[30]

Experimental Section

General: All manipulations were performed using standard Schlenk or dry box techniques and a dinitrogen or argon atmosphere (H_2O and $O_2 <$ 1 ppm). Apparatus were closed by J. Young valves with a glass stem (leak-tight at −80 °C). All solvents were rigorously dried over P_2O_5 and degassed prior to use and stored under N_2. I_2 and P_4S_3 were obtained from commercial sources and purified prior to use by sublimation or recrystallization from CS_2. $P_4S_3I_2$ was prepared by reacting P_4S_3 and iodine in CS_2 and its purity was checked by Raman spectroscopy.[1,21] $Ag[Al(OR)_4]$[4] and $Ag(P_4S_3)_2^+[Al(OR)_4]^-$[31] were prepared according to the literature. Raman and IR spectra were recorded using a 1064 nm laser on a Bruker IFS 66v spectrometer. IR spectra were recorded in Nujol mull between CsI plates. NMR spectra of sealed samples were run on a Bruker AC250 and Bruker AVANCE 400 spectrometer in CD_2Cl_2 and were referenced against the solvent (^1H, ^{13}C) or external H_3PO_4 (^{31}P), $CFCl_3$ (^{19}F) and aqueous $AlCl_3$ (^{27}Al). Measurements carried out in $C_6H_5CF_3$ were referenced towards a lock-capillary with d^8-THF. The ^{31}P NMR spectra were simulated and assigned with the programs WINNMR and WINDAISY[32] as well as NUMMRIT[33] for $P_7S_6I_2^+$ (Isomer II).

Syntheses of $P_7S_6I_2^+[Al(OR)_4]^-$:

Reaction between $Ag(P_4S_3)_2^+[Al(OR)_4]^-$ and $2I_2$: $Ag(P_4S_3)_2^+[Al(OR)_4]$ (0.969 g, 0.639 mmol) and I_2 (0.325 g, 1.279 mmol) were transferred under inert atmosphere into a two-bulbed vessel incorporating a fine sintered glass frit plate and closed by Young valves with a glass stem. CH_2Cl_2 (10 mL) and CS_2 (5 mL) were condensed onto the mixture at −78 °C. At this temperature the reaction proceeded very slowly. At −30 °C about half of the reacted diiodine was consumed in a relatively short time. It took one week for all visible amounts of I_2 to be consumed. After this time the only solid that remained in the flask was AgI. The solution was filtered through the frit-plate, highly concentrated and crystallized at −28 °C. The first crystals obtained were $P_5S_2I_2^+[Al(OR)_4]^-$ (0.070 g). After several months $P_7S_6I_2^+[Al(OR)_4]^-$ was obtained as large yellow plates (0.160 g, 15.5 %). The microcrystalline material obtained in this reaction was also used for the preparation of an NMR sample in $C_6H_5CF_3$ (with a $[D_8]$THF capillary). The sample decomposed within two days with P_4S_3, I_2, and PF_3 separation. ^{13}C NMR (63 MHz, CD_2Cl_2, −70 °C): δ = 120.6 (q, $J_{C,F}$ = 292.4 Hz; CF_3), 79.0 ppm (m; $C_{tert}(CF_3)_3$); ^{27}Al NMR (78 MHz, CD_2Cl_2, −50 °C): δ = 38.3 ppm (s, $\nu_{1/2}$ = 86.0 Hz).

Reaction between $Ag[Al(OR)_4]$ and 2 β-$P_4S_3I_2$: In a glove box, $Ag[Al(OR)_4]$ (0.995 g, 0.925 mmol) and β-$P_4S_3I_2$ (0.875 g, 1.850 mmol) were placed into a two-bulbed vessel connected through a frit plate and closed with two Young valves (with a glass stem). CH_2Cl_2 (10 mL) was condensed onto the mixture at −78 °C. The reaction started immediately with precipitation of the AgI resulting in a yellow to orange colored solution. The flask was left at −80 °C for at least two days, until all AgI precipitated, and additionally kept for about seven days at −30 °C. After this period of time the reaction mixture could be handled at room temperature: the solution was filtered from the solids, concentrated to an almost oily phase and crystallized at −30 °C. Large yellow plates of **4** were obtained in almost quantitative yield. The solid compound is thermally stable at room temperature, but very sensitive to air and moisture. They only survived about 1–2 min. at room temperature in PFE oil upon crystal mounting.

Reaction between $Ag[Al(OR)_4]$ and 2 β-$P_4S_3I_2$, NMR-scale experiment: In a glove box, $Ag[Al(OR)_4]$ (0.059 g, 0.044 mmol) and β-$P_4S_3I_2$ (0.041 g,

0.089 mmol) were placed into a NMR tube attached to a valve. Shortly before the measurement, CD_2Cl_2 (1.0 mL) was condensed onto the mixture at −78 °C. On shaking the tube (−78 °C), the reaction started immediately with precipitation of the AgI resulting in a yellow-to-orange colored solution. The sample was kept at −80 °C between the first and the second measurement and at −30 °C (two days) and at 0 °C (five days) before the third and the fourth measurements. The ^{13}C NMR spectra for all NMR tube experiments were recorded at the last stage of the reaction. ^{31}P NMR data are included in the tables in the main text. ^{13}C NMR (63 MHz, CD_2Cl_2, RT): δ = 121.4 ppm (q, $J_{C,F}$ = 292.1 Hz; CF_3).

X-ray crystal structure determination: Data collection for X-ray structure determinations were performed on a STOE IPDS II diffractometer using graphite-monochromated $Mo_{K\alpha}$ (0.71073 Å) radiation. Single crystals were mounted in perfluoroether oil on top of a glass fiber and then brought into the cold stream of a low-temperature device so that the oil solidified. All calculations were performed on PCs using the SHELX97 software package. The structure was solved by direct methods and successive interpretation of the difference Fourier maps, followed by least-squares refinement, see the following note for details.[34] One of two $P_7S_6I_2^+$ ions in the asymmetric unit was disordered over two positions with an occupation of 66% for the main orientation. Both occupations were included anisotropically in the refinement. All CF_3 groups of the two independent anions were split over two positions (70% main occupation) and had to be fixed with SADI or DFIX/DANG restraints. All disordered positions were included in the refinement anisotropically. CCDC-259931 contains the supplementary crystallographic data for this paper. These data can be obtained free of charge from The Cambridge Crystallographic Data Centre via www.ccdc.cam.ac.uk/data_request/cif.

Computational details: The majority of the computations were performed with the program TURBOMOLE.[35,36] The geometries of all species were optimized at the (RI-)MP2 level[37] with the triple ζ valence polarization (two d and one f functions) TZVPP basis set.[38,39] The 28 and 46 electron cores of Ag and I were replaced by a quasirelativistic effective core potential.[40] All species were also fully optimized at the BP86/SV(P) (DFT-)level, though these geometries are not shown. Approximate solvation energies (CH_2Cl_2 solution with ε_r = 8.93) were calculated with the COSMO model[41] at the BP86/SV(P) (DFT-)level using the MP2/TZVPP geometries. Frequency calculations were performed for all species and structures represent true minima without imaginary frequencies on the respective hypersurface. For thermodynamic calculations, the zero point energy and thermal contributions to the enthalpy and the free energy at 298 K have been included.[42] The calculation of the thermal contributions to the enthalpy and entropic contributions to the free energy were performed using TURBOMOLE and the FreeH module. For all species a modified Roby–Davidson population analysis based on occupation numbers (paboon) was performed using the (RI-)MP2/TZVPP electron density. The calculation of chemical shifts and spin–spin coupling constants was done with Gaussian 03 at the MPW1PW91/6–311G(2df) level of theory (i.e. using the keyword nmr = spinspin) with fully optimized structures obtained at the same level.[43] The MPW1PW91/6–311G(2df) level was selected, since it has previously reproduced quantum chemical problem cases like the S_4^{2+} and S_8^{2+} cations.[44–46] The referencing of calculated chemical shifts was done in analogy to the procedure described by B. Tattershall[22] with the only difference that all halogen-bearing atoms, which are known to be systematically in error due to relativistic effects,[24] were omitted for the assignment of the reference values. Since the reference values for the three isomers of $P_7S_6I_2^+$ were the same within 1.3 ppm (290.2 (I), 288.9 (II), and 290.2 ppm (III)), we used the same reference point for $\delta^{31}P$ = 0 ppm of (290.2 + 288.9 + 290.2)/3 = 289.8 ppm for the absolute isotropic shielding tensor. The reference point for sulfonium $P_4S_3Br^+$ is 305.6 ppm, for dibromophosphonium $P_4S_3Br_3^+$ it is 287.7 ppm. All calculated chemical shifts and coupling constants are deposited together with machine-readable *xyz* orientations of the calculated structures and the calculated vibrational frequencies.

Acknowledgements

This work was supported by the Deutsche Forschungsgemeinschaft, the Fonds der Chemischen Industrie, the Universität Karlsruhe (TH), and the EPF Lausanne.

[1] G. M. Sheldrick, G. J. Penney, *J. Chem. Soc. A* **1971**, 1100–1103.
[2] S. Brownridge, I. Krossing, J. Passmore, H. D. B. Jenkins, H. K. Robottom, *Coord. Chem. Rev.* **2000**, *197*, 397–481.
[3] C. Aubauer, G. Engelhardt, T. M. Klapötke, A. Schulz, *J. Chem. Soc. Dalton Trans.* **1999**, 1729–1734.
[4] I. Krossing, *Chem. Eur. J.* **2001**, *7*, 490–502.
[5] M. Gonsior, I. Krossing, *Dalton* **2005**, 1203–1213.
[6] M. Gonsior, I. Krossing, E. Matern, *Chem. Eur. J.* **2006**, *12*, DOI: 10.1002/chem.200500138.
[7] I. Krossing, A. Bihlmeier, I. Raabe, N. Trapp, *Angew. Chem.* **2003**, *117*, 1569–1572; *Angew. Chem. Int. Ed.* **2003**, *42*, 1531–1534.
[8] M. Gonsior, I. Krossing, L. Müller, I. Raabe, M. Jansen, L. Van Wüllen, *Chem. Eur. J.* **2002**, *8*, 4475–4492.
[9] I. Krossing, *J. Chem. Soc. Dalton Trans.* **2002**, 500–512.
[10] I. Krossing, I. Raabe, *Angew. Chem.* **2001**, *113*, 4544–4547; *Angew. Chem. Int. Ed.* **2001**, *40*, 4406–4409.
[11] M. Gonsior, I. Krossing, *Chem. Eur. J.* **2004**, *10*, 5730–5736.
[12] I. Krossing, I. Raabe, *Angew. Chem.* **2004**, *116*, 2116–2142; *Angew. Chem. Int. Ed.* **2004**, *43*, 2066–2090.
[13] D. Gudat, *Eur. J. Inorg. Chem.* **1998**, 1087–1094.
[14] A. H. Cowley, R. A. Kemp, *Chem. Rev.* **1985**, *85*, 367–382.
[15] T. B. Huang, L. F. Liu, X. L. Xu, W. F. Huang, K. Wang, *Chin. Chem. Lett.* **1999**, *10*, 205–206.
[16] T. B. Huang, J. L. Zhang, C. G. Zhan, Y. J. Zhang, *Sci. China Ser. B* **1993**, *36*, 641–648.
[17] N. Burford, B. W. Royan, J. M. Whalen, J. F. Richardson, R. D. Rogers, *J. Chem. Soc. Chem. Commun.* **1990**, 1273–1275.
[18] B. H. Christian, R. J. Gillespie, J. F. Sawyer, *Inorg. Chem.* **1981**, *20*, 3410–3420.
[19] K. Stumpf, R. Blachnik, G. Roth, G. Kastner, *Z. Kristallogr. New Crystal Structures* **1999**, *214*, 399–400.
[20] A. Koblischek, H. A. Hausen, J. Weidlein, H. Binder, *Z. Naturforsch. B: Chem. Sci.* **1983**, *38*, 1046–1053.
[21] a) A. W. Cordes, G. W. Hunt, *Inorg. Chem.* **1971**, *10*, 1935–1938; b) R. Blachnik, U. Rabe, *Z. Anorg. Allg. Chem.* **1980**, *461*, 87–90.
[22] B. W. Tattershall, R. Blachnik, A. Hepp, *Dalton Trans.* **2000**, 2551–2558.
[23] B. W. Tattershall, N. L. Kendall, *Polyhedron* **1994**, *13*, 1517–1521.
[24] M. Kaupp, C. Aubauer, G. Engelhardt, T. M. Klapötke, O. L. Malkina, *J. Chem. Phys.* **1999**, *110*, 3897–3902.
[25] Parameters for Br···F, I···F and P···F contacts are not available.
[26] T. J. Wentink, *J. Phys. Chem.* **1958**, *29*, 188–200.
[27] I. Raabe, A. Reisinger, N. Trapp, I. Krossing, unpublished results.
[28] Since β-$P_4S_3I_2$ appears not to react with Ag^+, we omitted the structures derived from β-$P_4S_3I_2$. They are deposited.
[29] A possible reason for our lack of success in obtaining crystals of isomer II is that asymmetrical species are less likely to crystallize. However, we observed that a new batch of crystals obtained from the reaction between β-$P_4S_3I_2$ and the silver salt, contains three independent (partly disordered) $P_7S_6I_2^+$ ions in the asymmetric unit. When isolated and dissolved in CD_2Cl_2 these crystals gave the same resonances of the three isomers of **4** as recorded in the in situ reaction. Thus, it is very likely that all three isomers can co-crystallize. However, we could not refine the structure to a publishable *R* value because various isomers occupy the same site and there is substantial disorder of the CF_3 groups of the $[Al(OR)_4]^-$ ions (*R*1 is currently at 20%).
[30] M. D. Chen, R. B. Huang, L. S. Zheng, Q. E. Zhang, C. T. Au, *Chem. Phys. Lett.* **2000**, *325*, 22–28.
[31] A. Adolf, M. Gonsior, I. Krossing, *J. Am. Chem. Soc.* **2002**, *124*, 7111–7116.

[32] a) Programs WINNMR and WINDAISY, Bruker Daltonic, Bremen, **1999**; b) G. Hägele, M. Engelhardt, W. Boenigk, *Simulation und automatisierte Analyse von NMR-Spektren*, VCH, Weinheim, **1987**.
[33] Program SpinWorks 2.4, K. Marat, University of Manitoba, ftp://davinci.chem.umanitoba.ca/pub/marat/SpinWorks; included program: NUMMRIT, R. A. Sebastian, K. Marat, modified version of NUMARIT, J. S. Martin, A. R. Quirt.
[34] Crystallographic details for $P_7S_6I_2^+[Al(OR)_4]^-$ (**4**): Crystal size $0.4\times0.1\times0.4$ mm, crystal system: triclinic, space group $P\bar{1}$, $a = 11.020(2)$, $b = 19.879(4)$, $c = 23.177(5)$ Å, $\alpha = 103.26(3)$, $\beta = 94.40(3)$, $\gamma = 100.18(3)°$, $V = 4827.7(17)$ Å^3, $Z = 4$, $\rho_{calcd} = 2.327$ Mg m^{-3}, $\mu = 2.061$ mm^{-1}, max./min. trans. = 0.3622/0.8356, $2\theta_{max} = 54.4°$, $T = 100$ K, 51892 reflections collected, 19892 unique reflections, 12967 reflections observed (2σ), R(int.) = 0.0637, GOOF/GOOF restrained = 1.075/1.074, final $R/wR2$ ($2(\sigma)$ = 0.0785/0.2256, final $R/wR2$ (all data) = 0.1071/0.2497, largest residual peak [e Å^{-3}] = 1.334.
[35] R. Ahlrichs, M. Bär, M. Häser, H. Horn, C. Kölmel, *Chem. Phys. Lett.* **1989**, *162*, 165–169.
[36] M. von Arnim, R. Ahlrichs, *J. Chem. Phys.* **1999**, *111*, 9183–9190.
[37] F. Weigend, M. Häser, *Theor. Chim. Acta* **1997**, *97*, 331–340.
[38] A. Schäfer, H. Horn, R. Ahlrichs, *J. Chem. Phys.* **1992**, *97*, 2571–2577.
[39] A. Schäfer, C. Huber, R. Ahlrichs, *J. Chem. Phys.* **1994**, *100*, 5829–5835.
[40] W. Kuechle, M. Dolg, H. Stoll, H. Preuss, *Mol. Phys.* **1991**, *74*, 1245.
[41] A. Klamt, G. Schürmann, *J. Chem. Soc. Perkin. Trans.* **1993**, *2*, 799–805.
[42] Thermal and entropic contributions to the enthalpy and free energy were obtained with TURBOMOLE software package.
[43] Gaussian 03, Version 6.0, M. J. Frisch, G. W. Trucks, H. B. Schlegel, G. E. Scuseria, M. A. Robb, J. R. Cheeseman, J. A. Montgomery, Jr., T. Vreven, K. N. Kudin, J. C. Burant, J. M. Millam, S. S. Iyengar, J. Tomasi, V. Barone, B. Mennucci, M. Cossi, G. Scalmani, N. Rega, G. A. Petersson, H. Nakatsuji, M. Hada, M. Ehara, K. Toyota, R. Fukuda, J. Hasegawa, M. Ishida, T. Nakajima, Y. Honda, O. Kitao, H. Nakai, M. Klene, X. Li, J. E. Knox, H. P. Hratchian, J. B. Cross, C. Adamo, J. Jaramillo, R. Gomperts, R. E. Stratmann, O. Yazyev, A. J. Austin, R. Cammi, C. Pomelli, J. W. Ochterski, P. Y. Ayala, K. Morokuma, G. A. Voth, P. Salvador, J. J. Dannenberg, V. G. Zakrzewski, S. Dapprich, A. D. Daniels, M. C. Strain, O. Farkas, D. K. Malick, A. D. Rabuck, K. Raghavachari, J. B. Foresman, J. V. Ortiz, Q. Cui, A. G. Baboul, S. Clifford, J. Cioslowski, B. B. Stefanov, G. Liu, A. Liashenko, P. Piskorz, I. Komaromi, R. L. Martin, D. J. Fox, T. Keith, M. A. Al-Laham, C. Y. Peng, A. Nanayakkara, M. Challacombe, P. M. W. Gill, B. Johnson, W. Chen, M. W. Wong, C. Gonzalez, J. A. Pople, Gaussian, Inc., Pittsburgh, PA, **2003**.
[44] H. D. B. Jenkins, L. C. Jitariu, I. Krossing, J. Passmore, R. Suontamo, *J. Comput. Chem.* **2000**, *21*, 218–226.
[45] T. S. Cameron, R. J. Deeth, I. Dionne, H. Du, H. D. Jenkins, I. Krossing, J. Passmore, H. K. Roobottom, *Inorg. Chem.* **2000**, *39*, 5614–5631.
[46] I. Krossing, J. Passmore, *Inorg. Chem.* **1999**, *38*, 5203–5211.

Received: February 9, 2005
Revised: September 20, 2005
Published online: January 10, 2006

